PARTICLE DIFFUSION DUE TO NONADIABATIC BEHAVIOR IN THE PLASMA SHEET

A

THESIS

Presented to the Faculty of the University of Alaska

in Partial Fulfillment of the Requirements

for the Degree of

Master of Science

By

Perry C. Gray, B.A.

Fairbanks, Alaska

May 1981

PARTICLE DIFFUSION DUE TO NONADIABATIC
BEHAVIOR IN THE PLASMA SHEET

RECOMMENDED:

Lou-Chang Lee

Wm. Chr. Stahel

Gary A. Gislason

Robert D. Sunderman

Chairman, Advisory Committee

Head, Space Physics and
Atmospheric Sciences Program

Director, Division of Geosciences

APPROVED:

K. B. Clarke

Vice Chancellor for Research and Advanced Study

May 6, 1981

Date

Abstract

In order to understand the dynamics of the plasma sheet, a numerical study of the nonadiabatic behavior of particles in a model field geometry is performed. The particle's magnetic moment is considered for various initial parameters, corresponding to various particle energies and degrees of field curvature. It is shown that the magnetic moment changes as the particle passes through the plasma sheet, and that the magnitude of the change is related to the curvature of the field at the middle of the plasma sheet. The relation of the magnitude of the change in magnetic moment to the particle's pitch and phase angles as it passes through the sheet is numerically resolved. The nature of the change is considered as a mechanism for pitch angle diffusion, and a diffusion calculation is performed for an assumed particle distribution.

Table of Contents

List of Figures

List of Tables

Acknowledgements

I would like to express my appreciation to those who in a very great way are responsible for this work, by affording a student the opportunity to perform it, however any tribute other than the final product seem inappropriate. I would like to thank my advisor, Syun Akasofu, one of the most tolerant men I have ever met, for the freedom to do the work my own way; also, L. C. Lee for valuable insight.

I would like to thank the Max C. Fleischmann Foundation for the generous support without which the numerical work presented here would not have been possible.

I. Introduction

Particle dynamics in the plasma sheet have been widely studied in an attempt to understand the collective plasma dynamics of the magnetotail. Figure 1 illustrates the region of the magnetosphere with which we are concerned. The plasma in the tail of the magnetosphere forms a 'neutral sheet' which supports a cross-tail current. Number densities in the plasma sheet are of the order of 5 cm^{-3}, as opposed to less than 1 cm^{-3} in the 'lobes' above and below the sheet. The magnitude of the magnetic field in the lobes is as great as an order of magnitude larger than in the midplane of the plasma sheet, and is more aligned along the magnetotail. The reason for this is that in the tail region the largest component of the magnetic field is a result of the cross-tail current supported by the plasma sheet.

Two general approaches for solutions have been taken by various authors. The first attempted to obtain analytic solution to the equations of motion for an assumed field geometry. Using this approach, approximate solutions have been found in the highly nonadiabatic limit by Speiser (1965) and Sonnerup (1971), and in the highly adiabatic limit by Stern and Palmadesso (1975) and Stern (1977). The second approach is to numerically integrate the equations of motion for a given model of the magnetic and electric fields. The numerical approach has been used to study particle trajectories for a number of assumed geometries by Speiser (1967), Cowley (1971), Eastwood (1977), Pudovkin and Tsyganenko

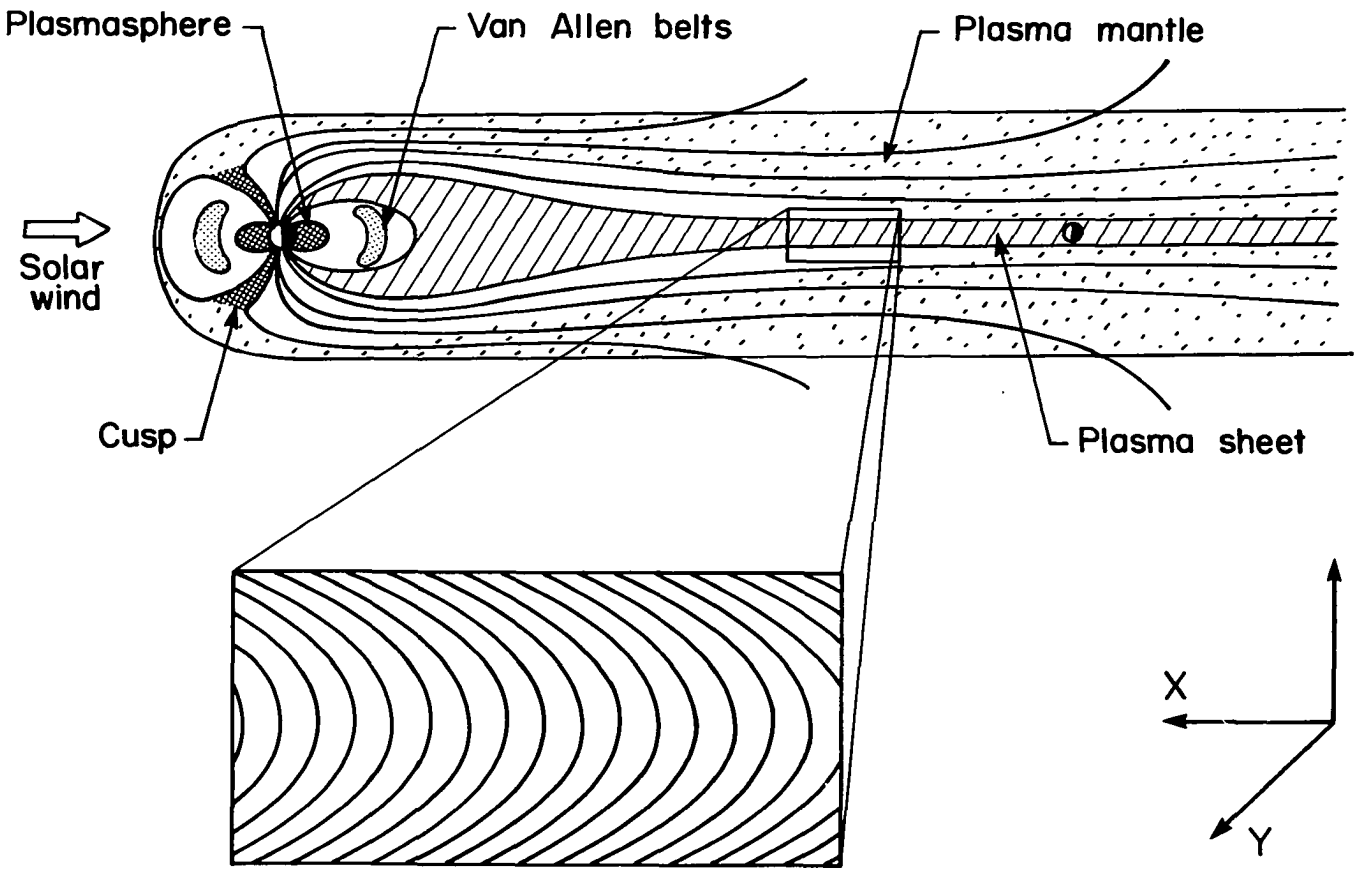

Figure 1.) Schematic drawing of the magnetosphere, enlarged area shows magnetic field for the sheet geometry.

(1973), and Swift (1977), and it has also been used by Wagner et al. (1979) in a comprehensive study.

Wagner et al. (1979) found that particle trajectories for the plasma sheet geometry fell into one of three categories. These three categories, corresponding to different degrees of nonadiabatic behavior near the midplane of the plasma sheet, may be classified by two parameters of the field geometry and particle energy. The first of these parameters is the scale length of inhomogeneity, which is the ratio of the characteristic length over which the field varies, spacially, to the size of the particle's gyroradius, and hence a function of both the field curvature and particle energy. The second parameter is the asymptotic ratio of the components of the magnetic field, in the assumed two-dimensional field model. The results of previous studies, Speiser (1967), Cowely (1971), Eastwood (1977), Pudovkin and Tsyganenko (1973), and Swift (1977), are consistent with this classification scheme.

In order to explain the particle dynamics in the plasma sheet geometry, we consider the nonadiabatic nature of the particles. By calculating the particle's magnetic moment, it is shown that the behavior, to a greater or lesser degree, depending on field curvature and particle energy, is nonadiabatic as the particle passes through the plasma sheet. By numerically resolving the effect of nonadiabatic behavior, for particular particle parameters at the middle of the plasma sheet, we determine the functional form for the change in the magnetic moment and consider this as a mechanism for noncollisional pitch angle

scattering. We then apply this mechanism to the problem of particle diffusion in the plasma sheet for an assumed particle distribution. The mechanism is also discussed as a possible mechanism by which oxygen ions may enter the ring current from the ionosphere.

The results obtained may also be used to explain the results of single particle studies for the reconnection geometry, Wagner et al. (1981). The effect limits those particles which reach the diffusion region by pitch angle scattering. A rough estimate of which particles may enter the diffusion region can be made from results from the sheet geometry.

The change in a particle's magnetic moment near a local minimum in the magnetic field has been studied previously by a number of authors, Grad and Van Norton (1962), Garren et al. (1958), Howard (1971), and Leffel ad Gray (1969). The general approach of these studies has been to study the nonadiabatic behavior of particles in a given field geometry, to determine an empirical form for the change in magnetic moment. Having an empirical form for the change in magnetic moment, an attempt is made to obtain an analytic approximation for the change in magnetic moment which agrees closely with the empirical form. Some success has been made with this technique, and a review and the most recent extension to the analytic approach may be found in Cohn, Rowlands and Foote (1977). The difficulty in applying the analytic approach to the plasma sheet geometry is that it requires an accurate representation of the field. The expressions which are used for the plasma sheet

geometry are not sufficiently accurate for this purpose; hence, we are limited to a numerical approach.

II. Normalization of the Equations of Motion and the Plasma Sheet Model

For our calculations we chose standard magnetospheric coordinates, with positive x towards the sun along the earth-sun line, positive y in the direction of the cross-tail current, and positive z normal to the midplane so as to complete a right handed coordinate system. We have, in general, for the equations of motion

$$m \frac{d\underset{\sim}{v}}{dt} = q \, (\underset{\sim}{E} + \underset{\sim}{v} \times \underset{\sim}{B}) \qquad (1.)$$

where $\underset{\sim}{v}$ is the particle velocity, $\underset{\sim}{E}$ is the electric field, $\underset{\sim}{B}$ the magnetic field, and q and m the particle charge and mass respectively. For the particle's gyroradius (ρ_{zo}) and gyroperiod (τ_o) :

$$\rho_o = \frac{mv_o}{qB_{zo}} \quad ; \quad \tau_o = \frac{m}{qB_{zo}}$$

where B_{zo} denotes the magnitude of the magnetic field at the point with respect to which we intend to normalize, for this case we assume it to be in the z direction, and v_o denotes the particle's initial velocity. If we normalize lengths to ρ_o and time to τ_o the equations of motion take on a numerically convenient form. We get

$$\frac{dv_x^*}{dt^*} = v_y^* B_z^* - v_z^* B_y^* + E_x^* \qquad (2.)$$

$$\frac{dv_y^*}{dt^*} = v_z^* B_x^* - v_x^* B_z^* + E_y^* \qquad (3.)$$

$$\frac{dv_z^*}{dt^*} = v_x^* B_y^* - v_y^* B_x^* + E_z^* \qquad (4.)$$

where $x^* = x/\rho_o$, $y^* = y/\rho_o$, $z^* = z/\rho_o$, $t^* = t/\tau_o$, $\underset{\sim}{v}^* = \underset{\sim}{v}/v_o$, $\underset{\sim}{B}^* = \underset{\sim}{B}/B_{zo}$ and $\underset{\sim}{E}^* = \underset{\sim}{E}/v_o B_{zo}$. The particle energy and the position with respect to which the normalization is performed may be chosen arbitrarily. The advantage of the normalization scheme described above is that particle behavior for a wide range of scale lengths and particle energies may be solved merely as a matter of finding the corresponding ratios, B^*, L^*, and t^*, for the given field geometry.

The model geometry which we chose for the plasma sheet is that used by Wagner et al. (1979) and is given by

$$\underset{\sim}{B} = B_{xo} \tanh (z/L)\, \hat{i} + B_{zo}\, \hat{k}$$

$$\underset{\sim}{E} = E_o\, \hat{j} \qquad (5.)$$

$$B_y = E_x = E_z = 0$$

where the scale length L can be thought of as the half thickness of the plasma sheet. The field model is similar to the two dimensional analytic solution for the plasma sheet by Kan (1973). While it is not a self-consistent solution of the Vlasov-Maxwell equations, it is adequate for single particle calculations. Using the normalization scheme outlined above we take $B_z^* = B_z/B_{zo} \equiv 1$ and for the equations of motion

we get

$$\frac{dv_x^*}{dt^*} = v_y^* \tag{6.}$$

$$\frac{dv_y^*}{dt^*} = v_z^* B_x^* - v_x^* + E_y^* \tag{7.}$$

$$\frac{dv_z^*}{dt^*} = - v_y^* B_x^* \tag{8.}$$

where

$$B_x^* = B_{xo}^* \tanh (z^*/L^*)$$

$$B_{xo}^* = B_{xo}/B_{zo} \quad ; \quad L^* = L/\rho_o$$

and

$$E^* = E_y/v_o B_{zo} = E_y^*$$

The z component of the magnetic field is constant; therefore, if we include the cross-tail electric field (E_y), we may use a special Lorentz transformation to a moving frame of reference in which there is no electric field. A discussion of the use of this transformation may be found in Speiser (1965) or Sonnerup (1971) . It is clear from the geometry that this frame moves with the velocity E_y/B_z in the positive x direction, so that the if v_o is the initial particle velocity in the rest frame and v_o' is the initial particle velocity in the moving

reference frame then we get

$$v_x^{*\prime} = v_x^* - E_y^* / B_{zo} \quad ; \quad v_y^{*\prime} = v_y^* \quad ; \quad v_z^{*\prime} = v_z^*$$

$$v_o' = [(v_x - E_y / B_z)^2 + v_y'^2 + v_z'^2]^{1/2} \qquad (9.)$$

and

$$\cos \alpha' = \frac{[\underset{\sim}{v} - (E_y/B)\,\hat{i}] \cdot \underset{\sim}{B}}{| \underset{\sim}{v}' | \, | \underset{\sim}{B} |}$$

where α' is the pitch angle in the moving frame. We may express a new special scaling gyroradius ρ_o', for the moving reference frame, in terms of v_o', v_o, and the scaling gyroradius in the rest frame ρ_o. The relation between L^* and $L^{*\prime}$ is then

$$L^{*\prime} = L^* (v_o / v_o') \qquad (10.)$$

When v_o' is larger than v_o, the effect of a cross-tail electric field is to decrease the scale length of inhomogeneity. Since the behavior for the case where there is a cross-tail electric field may easily be determined from the case where there is no electric field, we restrict our study to the latter case.

III. Field Curvature and the Nondimensional Magnetic Moment

As will be shown, the degree of nonadiabatic behavior a particle in the plasma sheet geometry exhibits is a function of the field curvature at the middle of the plasma sheet. An analytic expression for the curvature is needed to resolve the functional dependence of the particle behavior. Starting with the relation for a field line in two dimensions for the normalized equations

$$\frac{dx^*}{B_x^*} = \frac{dz^*}{B_z^*} \tag{11.}$$

or since $B_z^* \equiv 1$, we have for x^* in terms of z^*

$$x^* = \int B_x^* \, dz^*$$

$$= \int B_{xo}^* \tanh \left(\frac{z^*}{L^*}\right) dz^* \tag{12.}$$

$$= B_{xo}^* L^* \ln \cosh \left(\frac{z^*}{L^*}\right) .$$

Then for a field line, taking y to be zero, we have

$$\underset{\sim}{r}(z^*) = \left(B_{xo}^* L^* \ln \cosh \left(\frac{z^*}{L^*}\right), \; 0 \; , \; z^* \right) \tag{13.}$$

so that we may denote the reparameterization of $\underset{\sim}{r}(z^*)$ by arc length s, as $\underset{\sim}{\delta}(s)$ (ie. $\underset{\sim}{\delta}(s) = \underset{\sim}{r}(z^*)$) where

$$s = h(z) \equiv \int_{-\infty}^{z} | \underset{\sim}{r}'(\rho) | \, d\rho \qquad (14.)$$

We have the curvature $\kappa(z^*)$ given by

$$\kappa(z^*) = | \underset{\sim}{\delta}''(s) | \qquad (15.)$$

and for the radius of curvature

$$R_c(z^*) = \frac{1}{\kappa(z^*)} \qquad (16.)$$

For $\underset{\sim}{\delta}''(s)$ we have

$$\underset{\sim}{\delta}''(s) = \frac{1}{| \underset{\sim}{r}'(z^*) |} \frac{d}{dz^*} \frac{\underset{\sim}{r}'(z^*)}{| \underset{\sim}{r}'(z^*) |} \qquad (17.)$$

where

$$\underset{\sim}{r}'(z^*) = (B_{xo}^* \tanh (\frac{z^*}{L^*}) , 0 , 1) \qquad (18.)$$

or evalutating equation (17) we get

$$\underset{\sim}{\delta}''(s) = (\frac{B_{xo}^*}{L^*} \frac{\operatorname{sech}^2(z^*/L^*)}{(B_{xo}^{*2} \tanh^2(z^*/L^*) + 1)^2} , 0 ,$$

$$- \frac{B_{xo}^{*2}}{L^*} \frac{\tanh (z^*/L^*) \operatorname{sech}^2(z^*/L^*)}{(B_{xo}^* \tanh^2(z^*/L^*) + 1)^2}) . \qquad (19.)$$

For the curvature we get

$$\kappa(z^*) = \frac{B_{xo}^*}{L^*} \frac{\operatorname{sech}^2 \frac{z^*}{L^*}}{(B_{xo}^{*\,2} \tanh^2 \frac{z^*}{L^*} + 1)^{3/2}} \qquad (20.)$$

Evaluating $\kappa(z^*)$ at $z^*=0$ we find that the radius of curvature at the middle of the plasma sheet is given by

$$R_c \Big|_{z^*=0} = \frac{L^*}{B_{xo}^*} \quad . \qquad (21.)$$

At the plasma sheet the radius of curvature is the ratio of the parameters in the classification scheme for particle trajectories in the plasma sheet, Wagner et al. (1979). Figure 2 shows the radius of curvature as a function of z^* for various choices of L^* with $B^* = 10.0$. The curvature of the field is a rapidly increasing function of the distance from the middle of the plasma sheet, even for large half-thicknesses of the sheet ($L^*=100.0$), as can be seen from Figure 2 .

The degree of a particle's adiabatic behavior can be defined in terms of the variation of approximate constants of motion, the adiabatic invariants. In principle there can be as many invariants as degrees of freedom in the system. However, for the most general case we are only assured of the particle's magnetic moment as an adiabatic invariant. Even though the plasma sheet geometry has the particle's bounce period as an invariant, it is computationally simpler and less ambiguous to define a nondimensional quantity which corresponds to the first

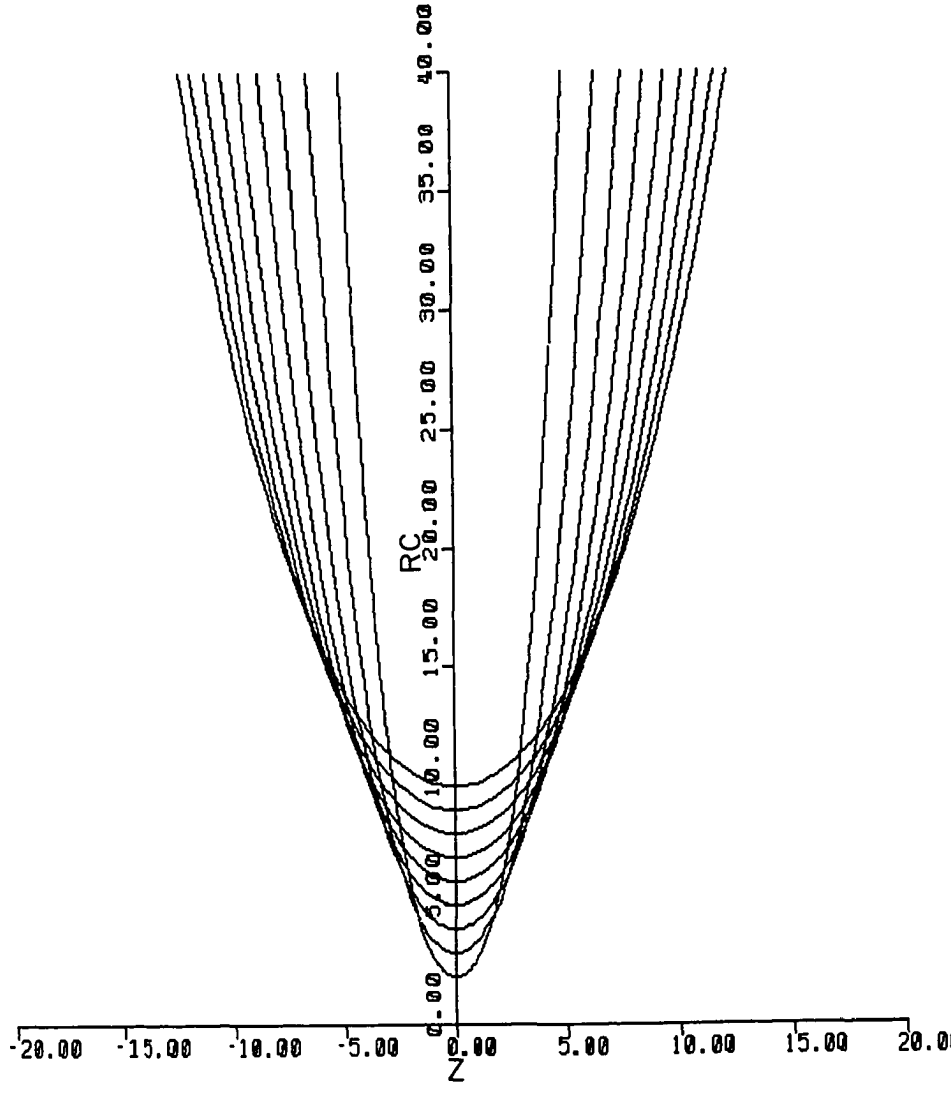

Figure 2.) The radius of curvature (R_c) for the plasma sheet geometry as a function of distance from the sheet z^* , for L^*= 20,30,40,50,60,70,80,90,100.

adiabatic invariant for the purpose of testing whether or not a particle's behavior is adiabatic.

The particle's magnetic moment is given by

$$\mu = \frac{1/2\, m\, v_{\perp}^{2}}{| B |} \tag{22.}$$

where $v_{\perp}$ must, in general, be evaluated in a frame moving with the guiding center velocity. If we are interested in maintaining first order accuracy then we will have

$$\mu = \frac{1/2\, m\, |\, (\underset{\sim}{v} - \underset{\sim}{u}_{E})\, |^{2} \sin^{2}\alpha}{| B (\underset{\sim}{r}_{gc}) |} \tag{23.}$$

where $\underset{\sim}{u}_{E}$ is the ExB drift ($\underset{\sim}{u}_{E} = \underset{\sim}{E} \times \underset{\sim}{B} / B^{2}$) , $\underset{\sim}{r}_{gc}$ is the guiding center position, and α is the particle pitch angle. Then in the nondimensional system we can define a normalized "magnetic moment"

$$\mu^{*} = \frac{1/2\, v^{*\,2} \sin^{2}\alpha}{B^{*}} \tag{24.}$$

where the magnitude of the magnetic field is $B^{*} = (B_{x}^{*\,2} + B_{z}^{*\,2})^{1/2}$. To correct for finite gyroradius effects the drift velcity and the magnitude of the magnetic field, B^{*}, must be evaluated at the guiding center position. It should be noted that since our system has no electric field, so that $v^{*} = 1 = \text{const.}$, and at the $z^{*} = 0$ plane μ^{*} reduces to

$$\mu^* = 1/2 \sin^2 \alpha \quad . \qquad (25.)$$

The nondimensional magnetic moment, at $z^*=0$, is strictly a function of the particle's pitch angle, regardless of the energy and lengths to which we scale the equations. This is particularly convenient since it will allow us to consider the behavior of a particle's magnetic moment in a single particle trajectory, and at the same time we will be able to use the information obtained to perform calculations for pitch angle scattering for a distribution of particle energies.

IV. Particle Trajectories and the First Adiabatic Invariant

Upon numerical integration, the equations of motion yield three characteristic types of trajectories. The trajectories vary with choice of field parameters, L^* and $B_{xo}{}^*$. For calculations in our study we have chosen to fix $B_{xo}{}^* = 10.0$, which corresponds to a geometry for the far plasma sheet (ie. B_{xo}=20.0 γ, B_{zo}=2.0 γ). For the case where $L^* > 100$ particles are strongly adiabatic and have a characteristic "folded figure eight" trajectory as shown in Figure 3. The particle is trapped and always passes through the plasma sheet with the same orientation, and as can be seen from the x-z projection, the particle bounces between symetrically situated mirror points. The displacement of the particle in the y direction as it passes through the midplane of the geometry is due to the curvature drift which is strongest there.

We can easily find when a particle will escape these trapped trajectories from the following loss condition for a mirroring particle,

$$E_o > \mu B_o \tag{26.}$$

where E_0 is the particle energy, B_0 is the maximum magnitude of the magnetic field and μ is the particle's magnetic moment ($\mu = \frac{1}{2} m v_\perp{}^2 / |B|$). For our nondimensional system the loss condition is

$$\mu^* < E_o{}^* / B_o{}^* \tag{27.}$$

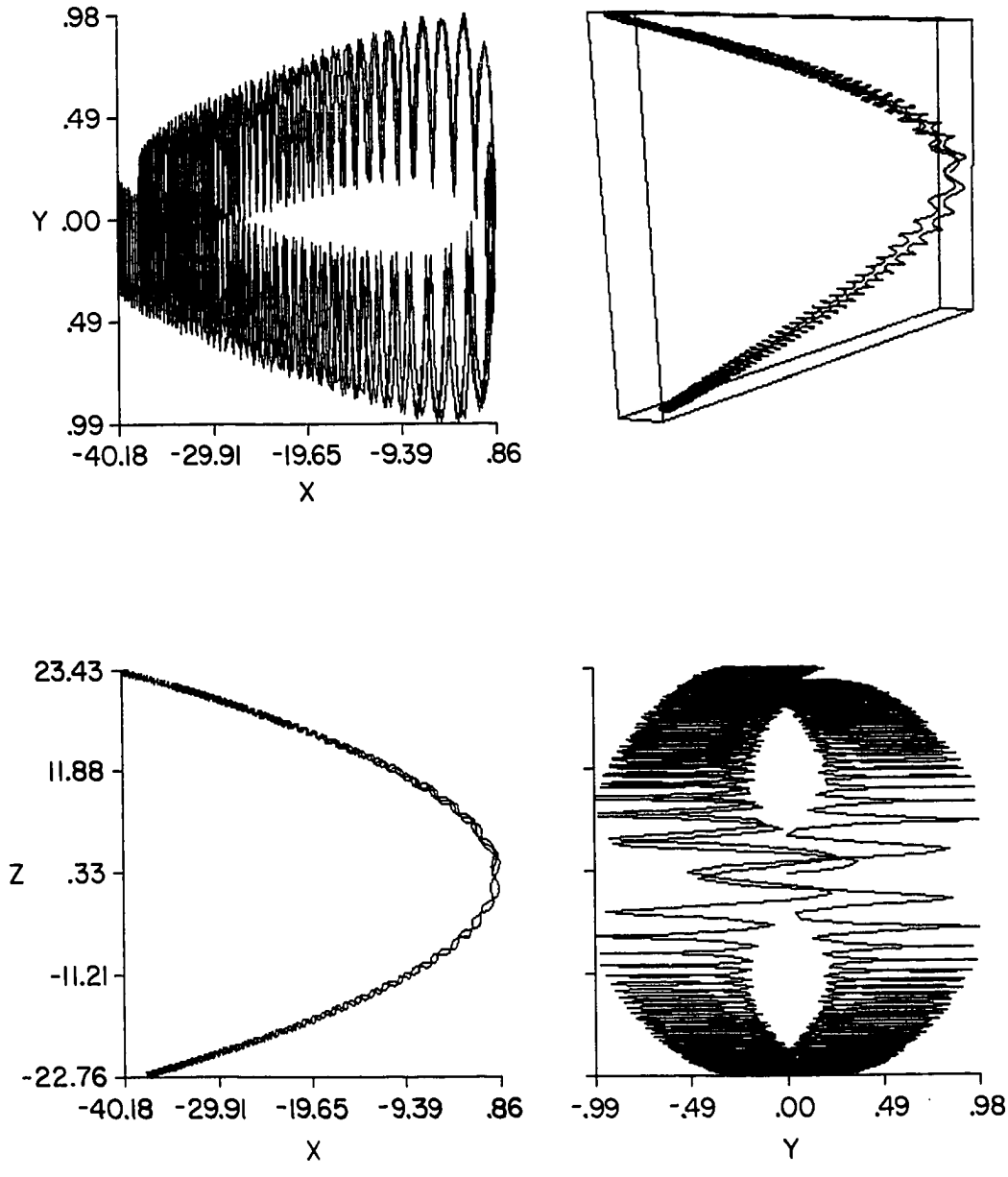

Figure 3.) Particle trajectory plot for a trapped particle in plasma sheet, particle performs "folded figure eight" trajectory, always passing through the sheet in the same direction (B^{*}=10.0 , L^{*}=65.0).

where

$$\mu^* = 1/2 \sin^2\alpha$$

$$E_o^* \equiv 1/2$$

and

$$B_o^* = (B^{*2} + 1)^{1/2}$$

where α is the pitch angle. For $B^* = 10.0$, we get

$$\mu^* < \frac{.5}{(101)^{1/2}} \sim .05$$

which correponds to a pitch angle of about 18^o at the plasma sheet.

The figure eight trajectory is the key behavior of particles in the plasma sheet. For values of $L^* \sim 50$ the particles have trajectories which show partially trapped behavior. They undergo several cycles of a figure eight trajectory, and then enter the loss cone and are ejected along the magnetic field. The trajectories for values of $L^* < 10$ show particle behavior which is highly nonadiabatic. The particle initially reaches the plasma sheet, oscillates about it several times and is then ejected along the magnetic field. These trajectories correspond to those calculated by Speiser (1967), and are essentially the limiting behavior for cases of either a very large initial particle energy or a very thin plasma sheet.

Figure 4 shows the magnetic moment for particle trajectories with three different choices of scale length, L^*. The apparent nonadiabatic

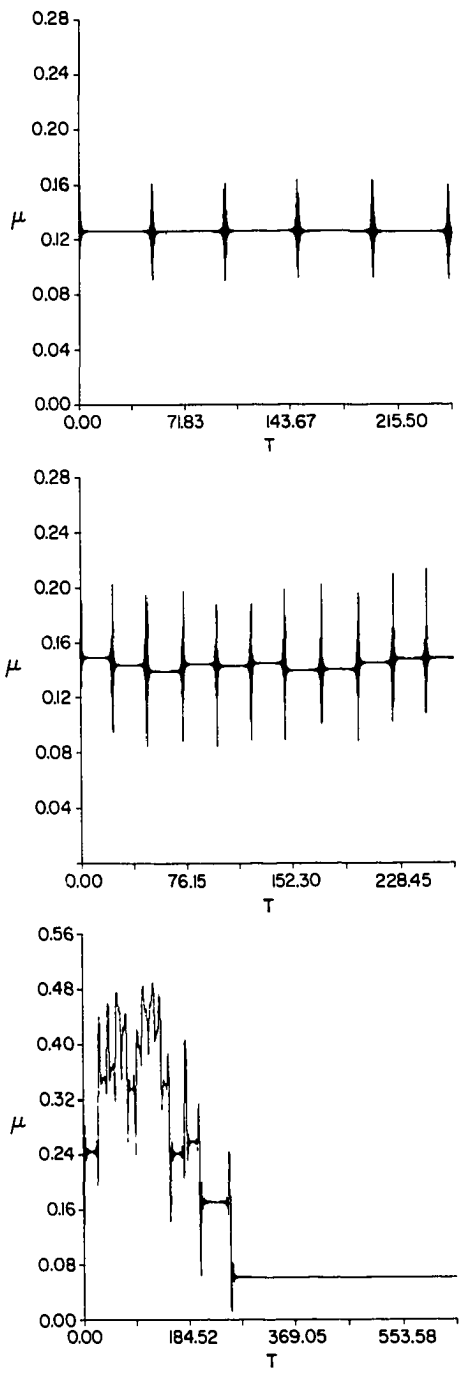

Figure 4.) The plot of μ^* vs. t^* for three particle trajectories; from top to bottom super-adiabatic slightly, and moderately nonadiabatic cases.

regions correspond to the particles' passage through the middle of the plasma sheet. The three figures demonstrate the transition from strongly adiabatic, trapped trajectories, to weakly adiabatic, partially trapped trajectories. The top figure is for $L^* = 100.0$, corresponding to a radius of curvature at $z^*=0$ of $R_c=10.0$, the particle behaves "super -adiabatically"; that is, the magnetic moment oscillates as it passes the midplane, but returns to its original value. The middle figure corresponds to the geometry of the trajectory shown in Figure 2 $L^* = 65.0$, or $R_c=6.5$ at $z^*=0$, there is an apparently random displacement of the magnetic moment as the particle passes through the middle of the plasma sheet. The bottom figure is for the case with $L^* = 20.0$, or $R_c=2.0$ at $z^*=0$, the change in magnetic moment as the particle passes through the midplane can be of the order of the magnetic moment, and the particle enters the loss cone after a few bounce periods. The behavior of the highly nonadiabatic particles is not of interest because they are lost from the plasma sheet in one transit of the sheet.

V. The Dependence of the Change in Magnetic Moment of the Field Curvature, Particle Pitch and Phase Angles at the Plasma Sheet

It is clear from the behavior of the particle's nondimensionalized magnetic moment, as demonstrated in Figure 4 , that particle behavior in the plasma sheet geometry is adiabatic except in some finite region centered on the middle of the plasma sheet, and the magnitude of the nonadiabatic effect is dependent on the scale length for the chosen geometry. In order to resolve the general form for the change in μ^* , a numerical study of the change in μ^* as a function of various field and particle parameters, at the $z^*= 0$ plane , was performed.

Figure 5 shows the results of the study of the change in μ^* as a function of field curvature at the middle of the plasma sheet. To compute values for the change, the particle pitch and phase angles are taken as fixed at the particle's initial position in the $z^*=0$ plane. The equations of motion are then pushed, first with a negative and then with a positive time step, yielding inital and final value for μ^* in the region on either side of the sheet where behavior is adiabatic. From Figure 5 it is clear that the form of the jump, in general, is

$$\Delta\mu = A(\alpha, \phi) \quad \exp\ [-\beta\ R_c] \qquad (28.)$$

where A (α,ϕ) a function of the particles pitch α , and phase ϕ at the middle of the plasma sheet, and R_c is the radius of curvature at the midplane of the sheet. Values for Figure 5 were calculated with fixed

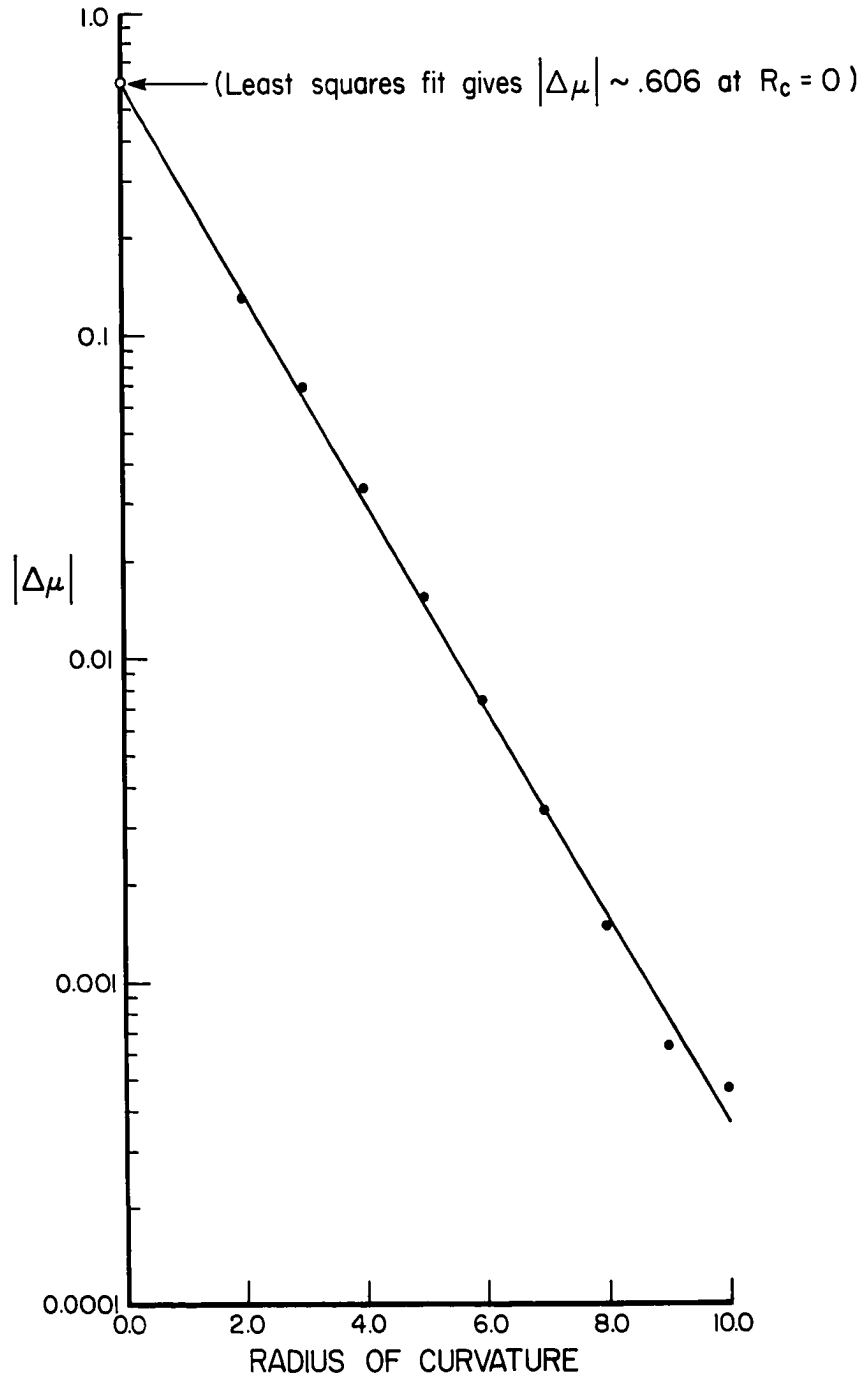

Figure 5.) The change in μ^* vs. R_c at the z=0 plane.

values of $B^*=10.0$, $\alpha_o= 30^o$ and $\phi_o=-90^o$, and with various values of scale length L^*. A numerical study of the effect of pitch and phase angle at the midplane of the plasma sheet on the exponential form of the change in magnetic moment has shown the form to be insensitive to these parameters, hence β in equation 28 may be taken as a constant to be determined below.

Having obtained an approximate general form for the change in μ^* it is necessary to resolve the effect of pitch and phase angles at the middle of the sheet, on the magnitude of the jump. Figure 6 shows the normalized change in μ^* as a function of the particle's magnetic moment at the $z^*=0$ plane. Values were calculated as above for a choice of $R_c=4.0$, at $z^*=0$, so as to insure a large enough change in μ^* to minimize error in the calculation of the jump. It can be seen that the maximum change in μ^* occurs for a value of $\mu^*\sim0.15$, which corresponds to a pitch angle of about 30^o at the midplane of the plasma sheet.

Figure 7 shows the results of the effect of the particles' phase angle at the middle of the plasma sheet on the magnitude of the jump in μ^*. Again calculations are done for a fixed field curvature, $R_c=4.0$, and initial pitch angle $\alpha=30^o$, at the middle of the plasma sheet. In our calculation a phase angle of 0^o at the $z^*=0$ plane corresponds to the perpendicular component of velocity being aligned in the positive y direction. As can be seen from Figure 7, the extreme changes in μ^* occur when the perpendicular velocity is aligned in either the positive or negative x direction, that is a phase angle of $\phi=90^o$.

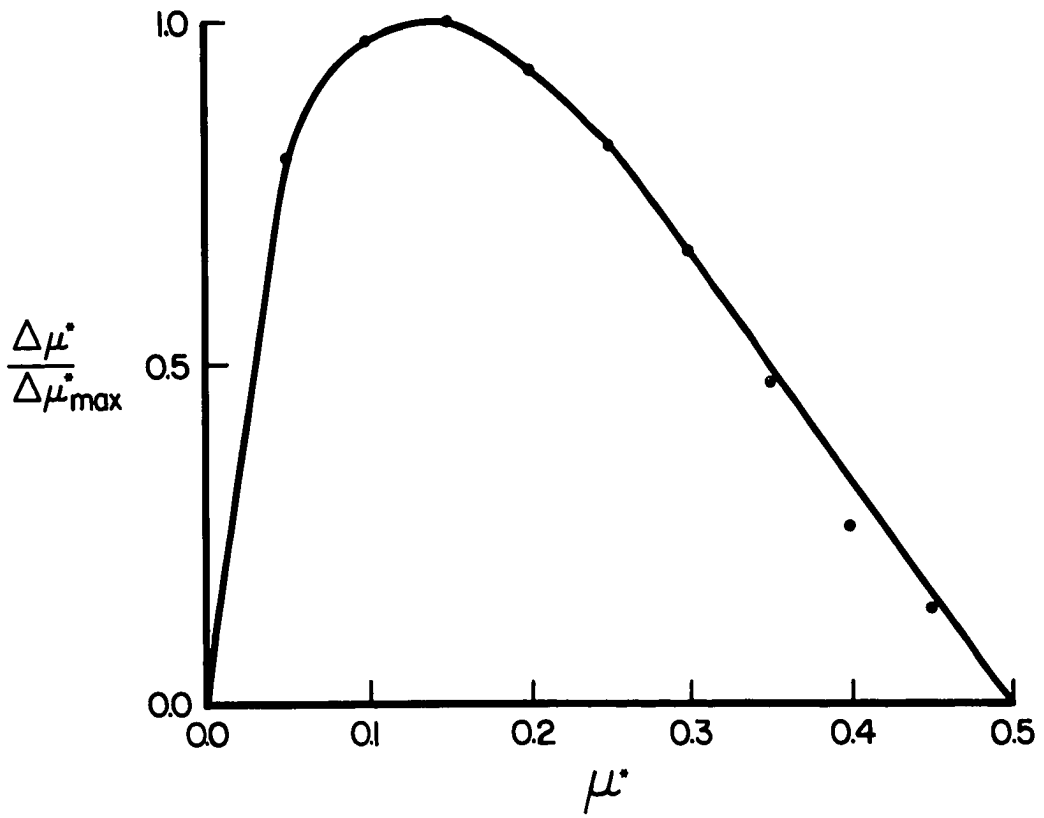

Figure 6.) The normalized change in μ^* ($|\Delta\mu/\Delta\mu_{max}|$) as a function of particle pitch angle or μ^* at the midplane (value calculated for $R_c|_{z=0} = 4.0$, $\phi_o = -90^o$).

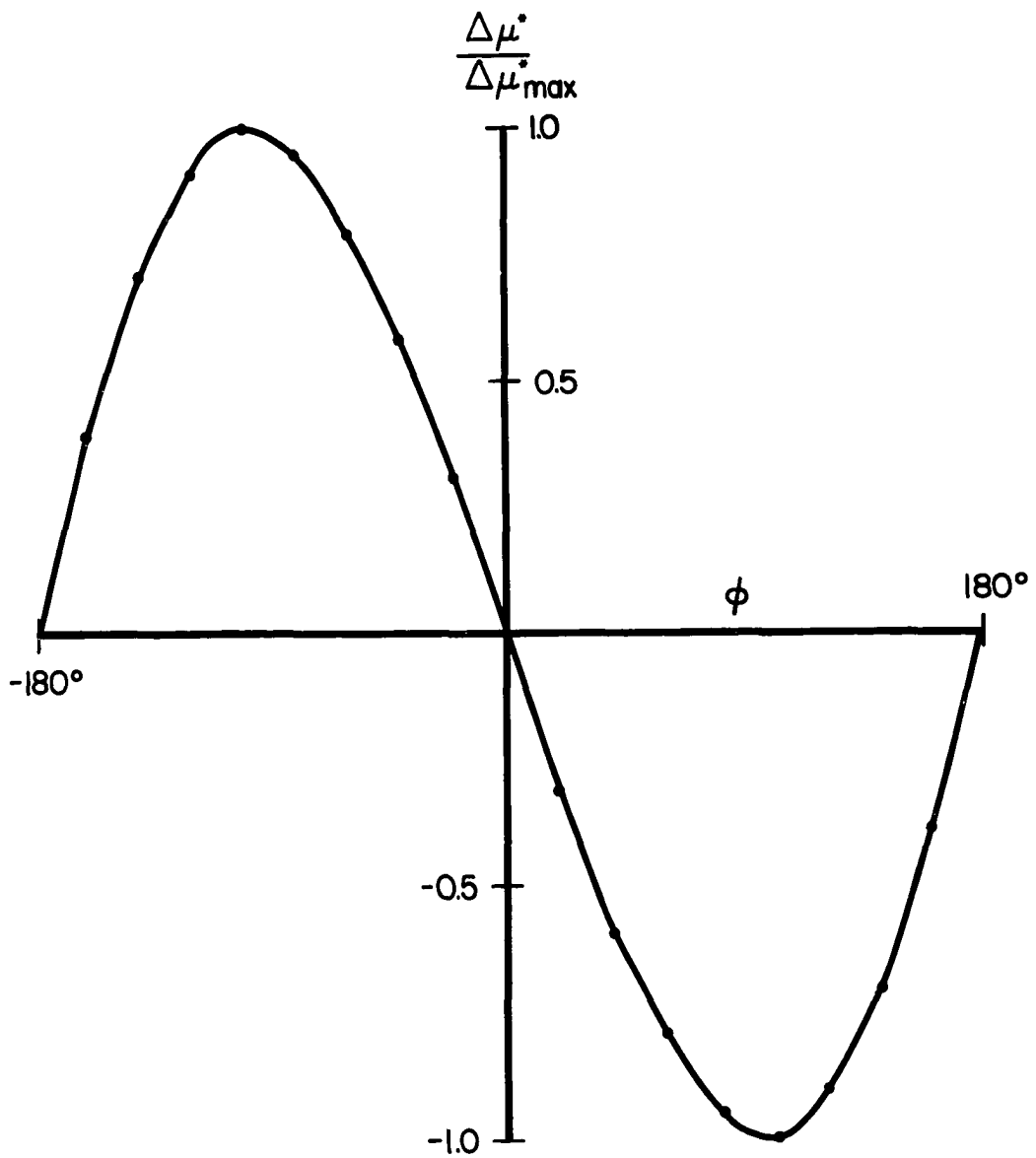

Figure 7.) The normalized change in μ^* ($\Delta\mu/\Delta\mu_{max}$) as a function of particle phase angle at the midplane (values calculated for $R_c|_{z=0} = 4.0$, $\alpha_o = 30^o$).

Knowing that the maximum change in μ^* occurs for a particle with a pitch angle of 30^o and a phase angle of 90^o at the middle of the plasma sheet, a linear regression analysis of the data for Figure 5 gives a maximum for A (α,ϕ), in equation (28), of 0.606, which may be obtained from the value for the y intercept. A value of -0.738 for β was obtained from the slope of the least squares fit to the data for Figure 5.

VI. Single Particle Diffusion in Magnetic Moment

The effect we have been studying can be considered as a mechanism for noncollisional pitch angle scattering. If we can determine the magnitude of the effect, it will be apparent whether the effect is significant compared to other loss proccess in the plasma sheet. With this in mind, we are initially interested in the time for a single particle to be lost by this mechanism. That is, given an initial field geometry, a scale length L^* and a limiting ratio of magnetic field strength $B_{xo}{}^*$ for a particle of a given energy, what is the time required for the pitch angle to be scattered a given amount.

We have, in general, for the diffusion coefficient

$$D_\mu = \frac{1}{2} \frac{< \Delta \mu^{*2} >}{\Delta t} \qquad (29.)$$

where D_μ is the diffusion coefficient for our proccess, and Δt is some characteristic time. For a single particle we are interested in the time for a particle with given initial parameters to enter the loss cone for a given geometry. This can be described as a classical one dimensional random walk proccess, where each passage of the particle across the sheet is an effective collision, and the mean time between events becomes the particle's half bounce. Then for a single particle it becomes an apparantly straight forward matter to calculate the diffusion coefficient as

$$D_{\mu} = \frac{1}{2N} \sum_{i=1}^{N} \frac{\Delta \mu_i^2}{\tau_i} \qquad (30.)$$

where τ_i is the i'th half bounce corresponding to the i'th crossing of the plasma sheet, in the given geometry.

Since the change in μ^* is a reasonably well behaved function of pitch, phase angles and field curvature at the sheet, as can be seen from Figures 5-7, it should be reasonably simple to handle these calculations numerically. However, τ^* (L^*, μ^* , ϕ) is not a readily determined function. In principle in order to compute a given τ^* it would require the integration of $v_{\parallel}$ along the field line from the midplane to the particles mirror point. Since μ^* at the mirror point does not correspond one to one with the values of μ^* at the midplane, it would require calculations of τ^* over the entire range of L^*, μ^*, and ϕ. At this point the number of calculations to resolve τ^*, for the numerical integration of D_{μ}, becomes prohibitively large.

Instead of attempting an exhaustive calculation for τ^* , we may make a gross approximation for the dependence of τ^* on pitch and phase angle by initially averaging over their effect. We are interested in the time it takes a particle of initial velocity v_o^* to leave a sheet of half thickness L^* . For a given value of L^*, we may calculate the quarter bounce period for a particle initially at its mirror point ($z_o^* = L^*$, $9/10\ L^* \ldots$; $\alpha_o = 90^o$) by determining the time the particle takes to reach the midplane. From these quarter bounce periods, we calculate an average half bounce with the effect of μ^*

averaged out. The particle's phase angle has little or no effect on the half bounce, other than the fact that the change in pitch angle is a function of value of the phase angle at the midplane, and we have averaged that effect. These approximations to the effect of μ^* and ϕ are not exact. However they are entirely sufficient for an order of magnitude calculation since what we require is a characteristic time scale for effective collisions. Having averaged out the dependence of τ^* on pitch and phase angle at the sheet we are left with τ^* as a function of L^* alone.

Using the approximation for τ^* the expression for the single particle diffusion coefficient, equation (30), may be easily evaluated numerically. Figure 8 shows the diffusion coefficient as a function of the radius of curvature at the midplane of the plasma sheet. The more rapidly decreasing function of the two plotted corresponds to the single particle calculation. For small values of the radius of curvature at the midplane, the diffusion coefficient is significantly large.

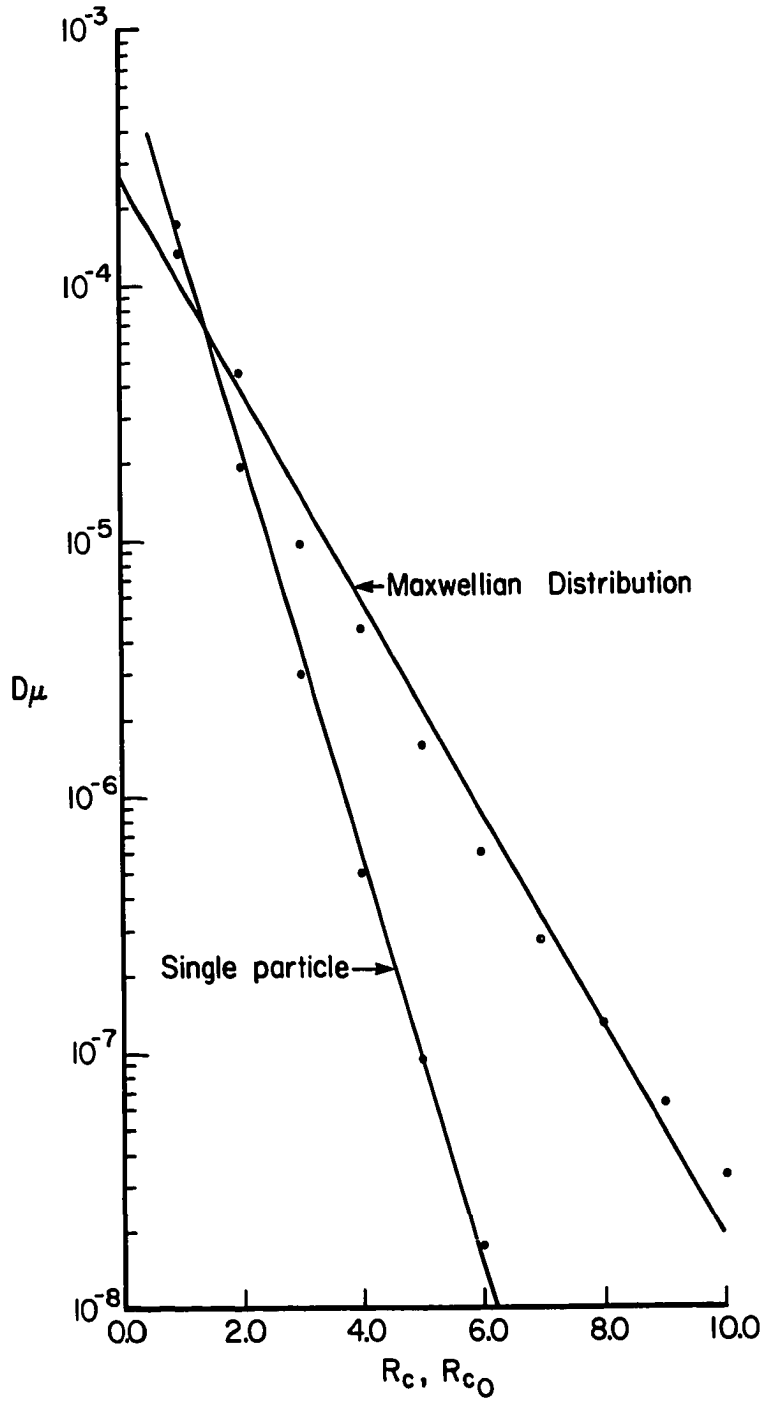

Figure 8.) D_μ vs. R_c for the single particle, and R_{co} for a Maxwellian distribution of particles.

VII. The Diffusion Calculation for an Assumed Particle Distribution

The single particle calculation presented previously is of interest for various reasons, particularly because it yields a result which, in principle, is easily verifiable numerically. However, we would like to be able to calculate a diffusion coefficient for the more general problem of a distribution of particle energies. The question we would like to answer is; given a plasma with initial pitch and phase angle distributions and a given energy distribution, what is diffusion like, due to this mechanism, as a function of mean energy.

Having numerically resolved an approximate form for the change in μ^*, we may perform diffusion calculations for a chosen particle distribution function. In particular, we will be concerned with a particle distribution which is an isotropic Maxwellian distribution. The choice of an isotropic phase and pitch angle distribution is reasonable since the effect we are examining may be considered as a mechanism for noncollisional pitch angle scattering.

A Maxwellian velocity distribution can be written as

$$f(\underset{\sim}{v}) = \frac{1}{\pi^{3/2} v_{th}^3} \exp\left[-\frac{v^2}{v_{th}^2}\right] \qquad (31.)$$

where v_{th} is the thermal velocity for the distribution. If we let $v_{th} = v_o$, then from our normalization scheme, we have

$$\frac{L^*}{L_o^*} = \frac{\dfrac{q\, B_{zo} L}{m\, v^*}}{\dfrac{q\, B_{zo} L}{m\, v_o^*}} = \frac{v^*}{v_o^*}$$

where L_o is the normalized scale length, corresponding to our choice of L and v_{th} . Since we may take $v_o^* \equiv 1$ in our normalization, we have

$$v^* = \frac{L_o^*}{L^*} \qquad (32.)$$

and our distribution function can be writen for the normalized system as

$$f\,(\mu^*, L^*) = \frac{1}{\pi^{3/2}} \exp\left[-\frac{L_o^{*2}}{L^{*2}}\right] \quad . \qquad (33.)$$

For the number density we must integrate the distribution function over velocity

$$n = \int f\,(\underset{\sim}{v}^*)\, d\underset{\sim}{v}^*$$

$$= \int\int 2\pi\, v_\perp^*\, f\,(v_\parallel^*, v_\perp^*)\, dv_\perp^*\, dv_\parallel^* \qquad (34.)$$

$$= \int\int 2\pi\, v_\perp^* J\,(L^*, \mu^*)\; f\,(v_\parallel^*, v_\perp^*)\, d\mu^*\, dL^*$$

where J is the Jacobian for the transformation from $v_\perp$ and $v_\parallel$ to μ^*

and L^*. Since there is no electric field we may write the nondimensionalized Hamiltonian as

$$H^* = 1/2\ v^{*2} \tag{35.}$$

$$= 1/2\ v_\perp^{*2} + 1/2\, v_\parallel^{*2} \quad .$$

We may write the parallel velocity as

$$v_\parallel^* = \frac{L_o^*}{L^*} (1 - 2\ \mu^*)^{1/2} \tag{36.}$$

since $v^* = L_o^*/\ L^*$, and $\mu^* = 1/2\ \sin^2\ \alpha$, and for the perpendicular velocity

$$v_\perp^* = \left(2 \frac{L_o^{*2}}{L^{*2}}\ \mu^* \right)^{1/2} \quad . \tag{37.}$$

The Jacobian is given by

$$J = \left| \begin{array}{cc} \frac{\partial\ v_\parallel}{\partial\ \mu^*} & \frac{\partial\ v_\parallel}{\partial\ L^*} \\ \frac{\partial\ v_\perp}{\partial\ \mu^*} & \frac{\partial\ v_\perp}{\partial\ L^*} \end{array} \right| = \frac{\sqrt{2}}{2}\ \frac{L_o^{*\,2}}{L^{*\,3}}\ (\mu^* - 2\ \mu^{*\,2})^{-1/2} \quad .$$

In order to get the mean value for some quantity in our nondimesional system we have merely to integrate over μ^* and L^* against this integrand.

In order to calculate the diffusion coefficient for the assumed particle distribution as a function of mean particle energy it is necessary to integrate $\Delta \mu^{*2}(L^*,\mu^*,\phi)$ against the distribution function. Then from the previous section we get for the diffusion coefficient

$$D_\mu = \frac{\iiint \frac{\Delta\mu^{*2}(L^*,\mu^*,\phi)}{\tau^*(L^*,\mu^*,\phi)} \frac{L_o^{*3}}{L^{*4}} \frac{\exp - [L_o^{*2}/L^{*2}]}{(1-2\mu^*)^{1/2}} dL^* d\mu^* d\phi}{\iiint \frac{L_o^{*3}}{L^{*4}} \frac{\exp - [L_o^{*2}/L^{*2}]}{(1-2\mu^*)^{1/2}} dL^* d\mu^* d\phi} \quad (40.)$$

where τ^* is again the half bounce of the particle as a function of L^*, ϕ and μ^*, where ϕ denotes the phase angle.

Using the approximation for τ^* from section VI, the diffusion coefficient for the assumed particle distributions can be numerically evaluated. Figure 8 shows the diffusion coefficient as a function of R_{co}, at $z^*=0$, for a Maxwellian distribution of particle energies where R_{co} corresponds to the radius of curvature at the midplane calculated from the scale length, L_o^*, for a particle with an initial velocity equal to the thermal velocity of the distribution. Both diffusion coefficients for the single particle case and the particle distribution are exponential in R_c, or R_{co} at the midplane. The two diffusion coefficients agree at small values of R_c, however the diffusion coefficient for the single particle case drops off much more rapidly than the diffusion coefficient for the distribution of particles. This

effect is to be expected since at small values of R_c the calculation of the diffusion coefficient for the distribution of particle energies reduces to the single particle case, that is the width of the distribution is small. At large values of R_{co} the more nonadiabatic particles in the distribution, that is those at higher energy, still make a significant contribution to the calculation, resulting in a larger diffusion coefficient than for the single particle calculation.

VIII. Discusion

The analysis of test particle trajectories for given magnetic field model is of use to give insight to particle dynamics. In general the results of such a study are limited in that they are incapable of resolving the plasma dynamics, since collective particle interactions and the effects of particle behavior on the fields are ignored. However, if we find some characteristic behavior in the particle dynamics of a given model, such as the nonadiabatic behavior in the plasma sheet geometry, we may get some idea of its importance from comparing magnitude of the effect with time and scale lengths for the system we are modeling.

A. The Degree of Nonadiabatic Behavior for Particles in the Plasma Sheet and Characteristic Loss Times for Ions

By considering typical values for the magnetic field and particle energies in the magnetotail, it is possible to get an idea of when effects of nonadiabatic behavior are significant. If we take B_{zo} in our field model to be 2 γ, as a typical value for the magnetic field at the midplane of the far plasma sheet and a range of half thicknesses from 1 to 6 R_E, we can calculate L^* for a given particle species of a given energy. Table 1 shows the normalized scale length L^* for ions of energy 6 KeV, and electrons of 1 KeV, typical values for the plasma sheet. If we assume that $B_{xo}^* = 10.0$, then it is readily apparent that the

Table 1.) Scale Length L^* for Typical Proton and Electron Energies in the Plasma Sheet, for Different L.

L (R_e)	L^* (6 KeV proton)	L^* (1 KeV electron)
1.0	1.14	119.49
2.0	2.28	238.98
3.0	3.42	358.47
4.0	4.55	477.96
5.0	5.67	597.45
6.0	6.83	716.94

$(B_{z_0} = 2.0\gamma,\ B^{\cdot}_{x_0} = 10.0;\ R_c\big|_{z=0} = L^{\cdot}/B^{\cdot}_{x_0})$

electrons will always behave super-adiabatically, since $R_c = L^*/B_{xo}^*$ at $z^* = 0$. On the other hand if $B_{xo}^* = 10.0$, corresponding to the far plasma sheet, the ion behavior is greatly affected by this mechanism.

If we consider a 6 KeV proton with an initial pitch angle of 45^o, in a geometry such that $L^*=10.0$, we see from the single particle diffusion coefficient that the particle loss time will be

$$t_{loss} = \frac{1}{2}\frac{(\sin 45)^2}{D_\mu(L^* = 10)} \approx 365\ \tau_o \quad . \qquad (41.)$$

Since τ_o for a 6 KeV proton in a 2 γ magnetic field is about 5 seconds the loss time is about 30 minutes. The loss times for particles in the Maxwellian distribution are comparable, since for small R_c the two diffusion coefficients agree more closely. The loss times are sufficiently short as to make this mechanism a significant loss process for particle in the plasma sheet.

We have shown that the nonadiabatic effects can apparently contribute to the loss of ions from the plasma sheet, but that the electrons are not affected. However, this does not imply that there will be charge separation. The ions which are lost from the plasma sheet will "drag" the electrons with them and the plasma will remain in a quasi-neutral state. Because of this, the diffusion time for the ions can be considered as the diffusion time for the plasma in the neutral sheet as a whole, due to nonadiabatic effects.

B. The Change in Magnetic Moment as a Possible Explanation of Single Particle Results for the Reconnection Geometry

We have previously carried out a single particle study for the reconnection geometry, Wagner et al. (1981). The equations for the model magnetic field for the reconnection geometry are given by

$$B_x = B_{xo} \tanh (z/L)$$

$$B_z = B_{zo} \tanh (x/L) \qquad (42.)$$

$$B_y = E_x = E_z \equiv 0$$

and

$$E_y = E_{yo} = \text{const.}$$

where L is the scale length of inhomogeneity for the magnetic field, as in the plasma sheet model. Figure 9 shows the magnetic field for this geometry. The model is a solution of the Vlasov-Maxwell equations for the special case where the separatricies are at right angles. It should also be noted that the ExB drift for a particle in the model field will be towards the neutral line when the particle is either above or below the neutral line, and away for the neutral line when it is on either side of it.

The relation of the reconnection model given above to the model for the plasma sheet becomes obvious if we consider the field at ¢x¢ > L or

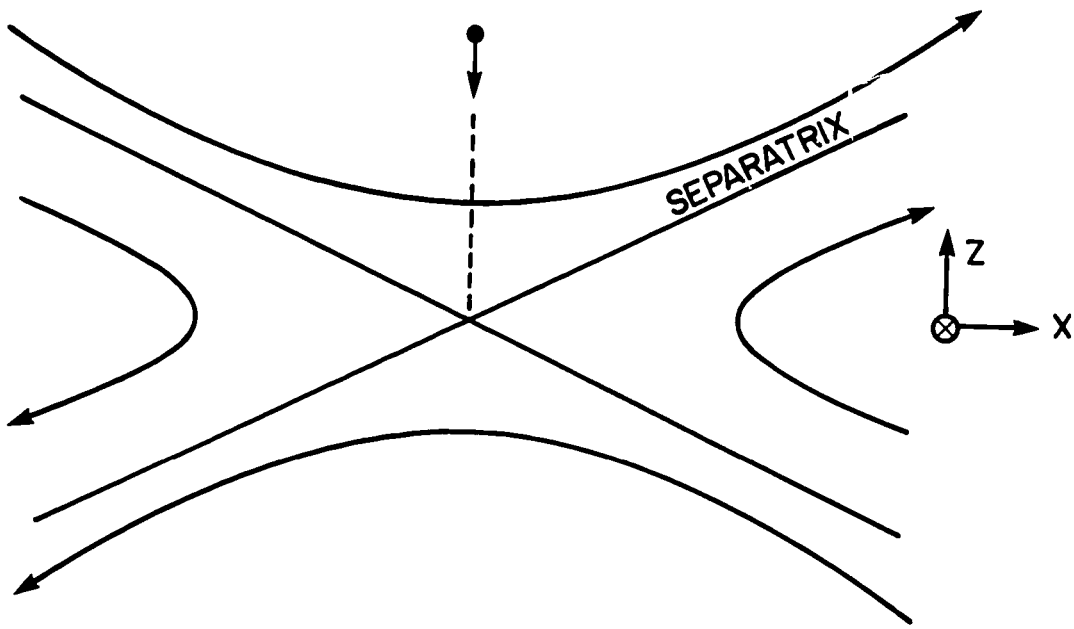

Figure 9.) The Reconnection Field Geometry

$|z| > L$. For example at large values of x the magnetic field reduces to

$$B_z \rightarrow B_{zo}$$

$$B_x = B_{xo} \tanh (z/L) \qquad (44.)$$

which are the equations for the plasma sheet geometry, used in the nonadiabatic study.

The same type of nondimensionalization scheme as given in section II may be applied to these model equations, however we may not transform away the electric field. Particle trajectories for the reconnection study were started directly over the nuetral line, usually with an initial z position greater than the scale length L. Figure 10 shows a typical trajectory for a particle in the reconnection geometry given above. The particle initially 'ExB drifts' down towards the neutral line, is displaced along the neutral line gaining a small amount of energy, then leaves the neutral line first along the x axis and then along the magnetic field. Closer study of the particle trajectories along with the behavior of the particles magnetic moment has shown that in the region near the y-z plane or the x-y plane, where the ExB drift is the greatest, the particle's behavior is analogous to the behavior in the plasma sheet geometry. The trajectory study showed that the greater percentage of particles started above the neutral line were lost before

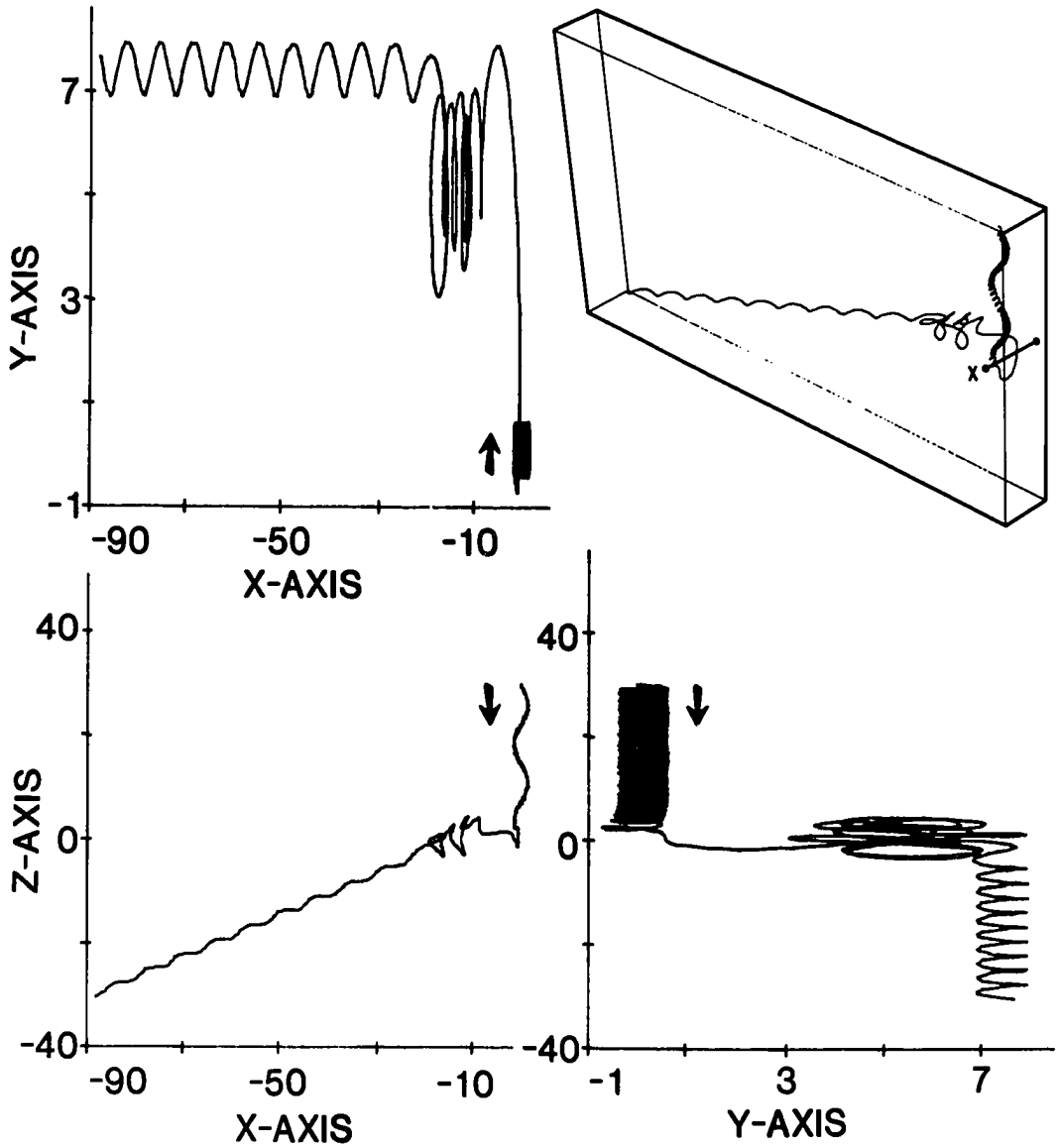

Figure 10.) Particle Trajectory for the Reconnection Field

reaching the neutral line. This result has been independently varified by a $2\,1/2$ dimensional particle simulation, Leboeuf et al. (1980).

The reason for the behavior described above, at least in the single particle calculation is easily understood. The length of time a particle takes to reach the neutral line is dependent only on the initial distance, z_o, from the neutral line and the magnitude of the ExB drift. If the geometry is such that the particles behavior above the neutral line is not super-adiabatic, then the condition to reach the neutral line is

$$t_{loss} = \frac{(\Delta \mu_{loss})^2}{2 D_\mu} > \frac{z_o}{v_{ExB}} . \qquad (45.)$$

The condition is simply that the time it takes a particle to reach the neutral line through ExB drift must be less than the time it takes the particle to be lost due to nonadiabatic effects. The expressions for $\Delta \mu$ and D_μ in equation 45 are those for the reconnection model, and would require extensive work to resolve numerically since both x and z components of the magnetic field vary with postion. If the particlular geometry for the initial position of the particle above the x-line is known an upper limic for the loss time of the particle may be calculated from the plasma sheet diffusion coefficient. Since the radius of curvature at the minimum in the magnetic field is a increasing function of distance above the neutral line an upper limit on the loss time for particle started above the neutral line may be obtained from the loss

condition for the neutral sheet geometry using the radius of curvature at the particle's initial height above the neutral line.

C. Analytic Approximations to the Change in Magnetic Moment

The fact that the magnetic moment of a particle in a mirroring geometry changes as the particle passes through a local minimum of the magnetic field has been known for some time Garren (1958). The effect has been studied for a number of different geometries, including cusped, Leffel and Gray (1969), and Howard (1971), and axially symmetric fields Garren et al. (1958).

One of the early attempts at an annalytic approximation for the change in the magnetic moment was made by Haste et al. (1969). Noting that the major contribution to the change in magnetic moment comes at the minimum of the magnetic moment they tried to evaluate

$$\Delta \mu = \int_{-t}^{t} \frac{\partial \mu}{\partial t} \, dt \qquad (46.)$$

where t=0 corresponds to the minimum in the magnetic field, and the range of integration is from mirror point to mirror point. Haste et al. tried to evaluate this integral by expressing the integrand in terms of phase averaged coordinates[see Bogoliubov and Zubarev (1955)], and solving by the method of steepest descent. Howard (1971) corrected the manner in which Haste et al. (1969) treated the poles of the integral by introducing the magnetic scalar potential into the integral for the

change in magnetic moment. The theory was extended to general three dimensional and non-vacuum fields by Cohn et al. (1978). They also give an overview of the application of the technique, and point out that the main difficulty in its aplication is the requirement for a sufficiently good expression for the magnetic field of interest. This renders the analytic approximation of limited use for particle behavior in fields where only an approximate expression is available.

IX. Conclusions

By considering the nonadiabatic nature of particles in the plasma sheet, we have shown that the classification scheme for particle trajectories in the plasma sheet proposed by Wagner et al. (1979), is consistent with the dependence of the degree of nonadiabatic behavior on the field curvature at the middle of the plasma sheet. The classification scheme is in terms of the ratio of the x component to the z component of the magnetic field, B_{xo}^*, and the nondimensional scale length L^*, while the radius of curvature at the midplane is the ratio of these two quantities, $R_c = L^*/B_{xo}^*$.

The nonadiabatic behavior may be seen as a mechanism for pitch angle scattering in the plasma sheet. Since the model equations for the magnetic field in the plasma sheet geometry are only approximate, we cannot compute the change in magnetic moment from the approximate analytic theory. However, we may resolve the form for the change in the magnetic moment numerically, as a function of the particle's pitch and phase angles and the radius of curvature for the field at the midplane. Having a form for the change in magnetic moment, we may use it to calculate pitch angle scattering in the plasma sheet and compute a diffusion coefficient for both a single particle of given energy and for an ensemble of particles of given energy distribution.

Comparing the diffusion for ions and electrons of typical plasma sheet energies in a typical geometry, we find that the electrons are always super-adiabatic, while the ions are strongly affected by this

mechanism. Loss times for ions in the plasma sheet geometry are on the order of an hour. We may explain the results of single particle calculations in the reconnection geometry in terms of losses by this mechanism.

We have examined the pitch angle scattering of particles in the plasma sheet geometry and considered it as a loss process for mirroring particles. Another aspect of nonadiabatic effects may be to consider the same process as a mechanism by which ions which are accelerated by the field aligned potential structure, out to the plasma sheet, may be captured and then enter the ring current under ExB drift.

We consider an oxygen ion which is accelerated up from the ionosphere with a small but finite pitch angle. In the near earth magnetic field, 10 R_E or less, which for the most part is dipolar, the ion would most likely travel along the field line and be lost to the ionosphere in the opposite hemisphere from which it started. However, if the ion is initially at high enough geomagnetic latitude, then the field line which it will follow will map into the plasma sheet. In this case, the particle may be pitch angle scattered by nonadiabatic effects. If the particle's pitch angle is scattered sufficiently that it is trapped in the plasma sheet, and if the loss time for the ion by the same mechanism is sufficiently long, then the particle may ExB drift into the near earth field where it's behavior will be super-adiabatic.

The fraction of ions which would be trapped by this mechanism is a function of the pitch angle and energy distributions, as well as the initial geomagnetic latitude of the ions. Figure 11 shows the radius of

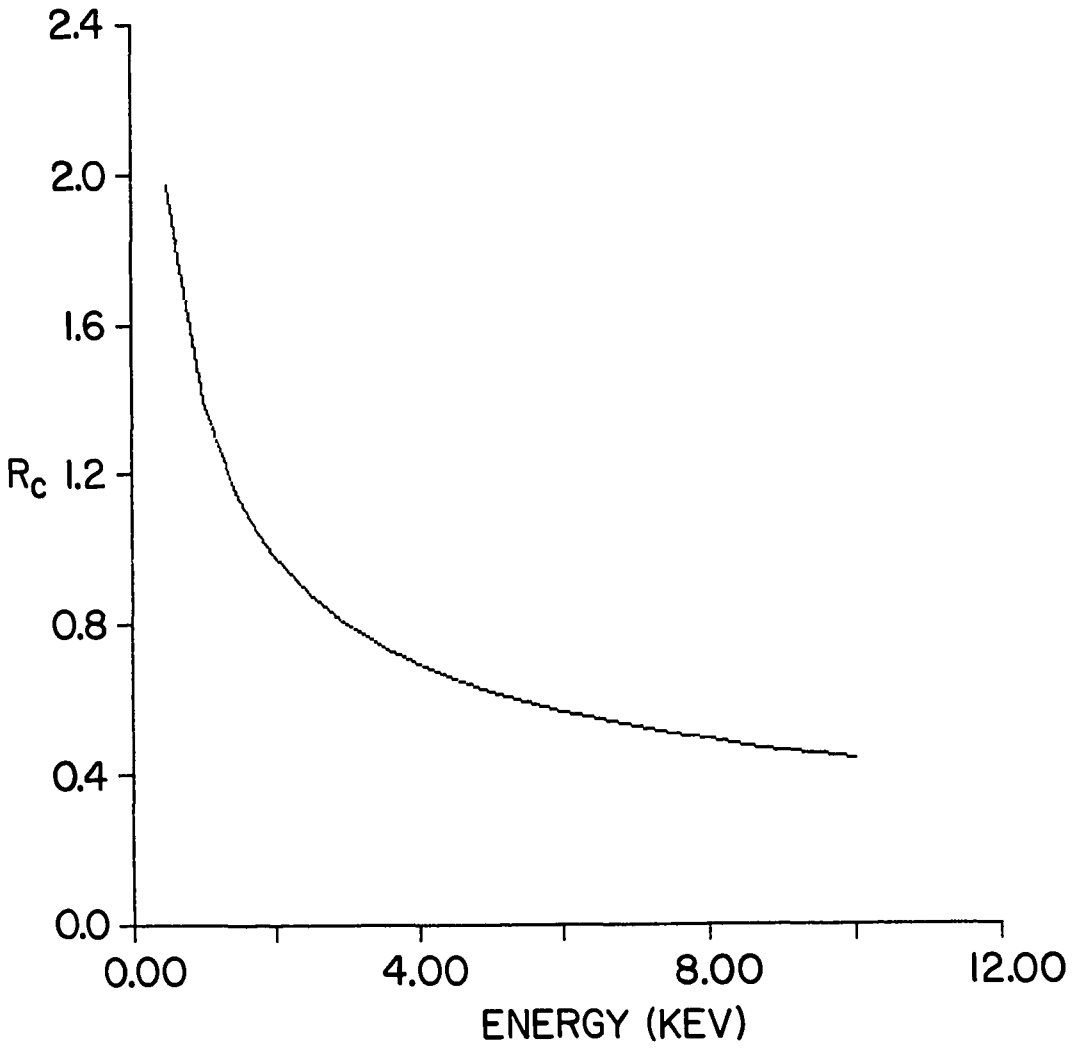

Figure 11.) The Radius of Curvature as a Function of Particle Energy for Oxygen Ions

curvature at the midplane of the plasma sheet geometry for oxygen ions, as a function of energy. The assumed geometry for the calculation is for a sheet half-thickness of 6 R_E , a z component of the magnetic field such that B_{zo}= 2 γ, and an asymptotic ratio of magnetic field components of B_{xo}^*= 1.0 . The value of B_{xo}^* corresponds to a limiting slope of 45^o for the field lines near the top or bottom of the modeled region. As can be seen from Figure 11, the magnitude of nonadiabatic effects is comparable to those for protons in the far plasma sheet. However, since the gyroperiod is linearly proportional to the mass of the particle, the loss time due to noadiabatic effects will be an order of magnitude longer for the oxygen ions. The radius of curvature at the midplane of the plasma sheet is a rapidly decreasing function of the distance down the magnetotail, so that oxygen ions in the region where B_{xo}^*>1.0 are likely to be readily lost from the sheet by nonadiabatic effects. Figure 12 shows a semi-quantitative model for the magnetic field in the magnetotail, Akasofu and Corrick (1980), under both quiet time conditions and disrupted conditions when part of the cross-tail current is diverted earthward along the magnetic field to the ionosphere. As can be seen, the region in which $B_{xo}^* \approx 1.0$ extends from 10 to 20 R_E, in the quite magnetosphere, which corresponds to the near edge of the plasma sheet.

The logical extension of this study would be an attempt at a numerical simulation of the plasma sheet. While the difference in the nonadiabatic effect on the loss of ions as opposed to electrons in the plasma sheet does not imply charge separation, it does imply a

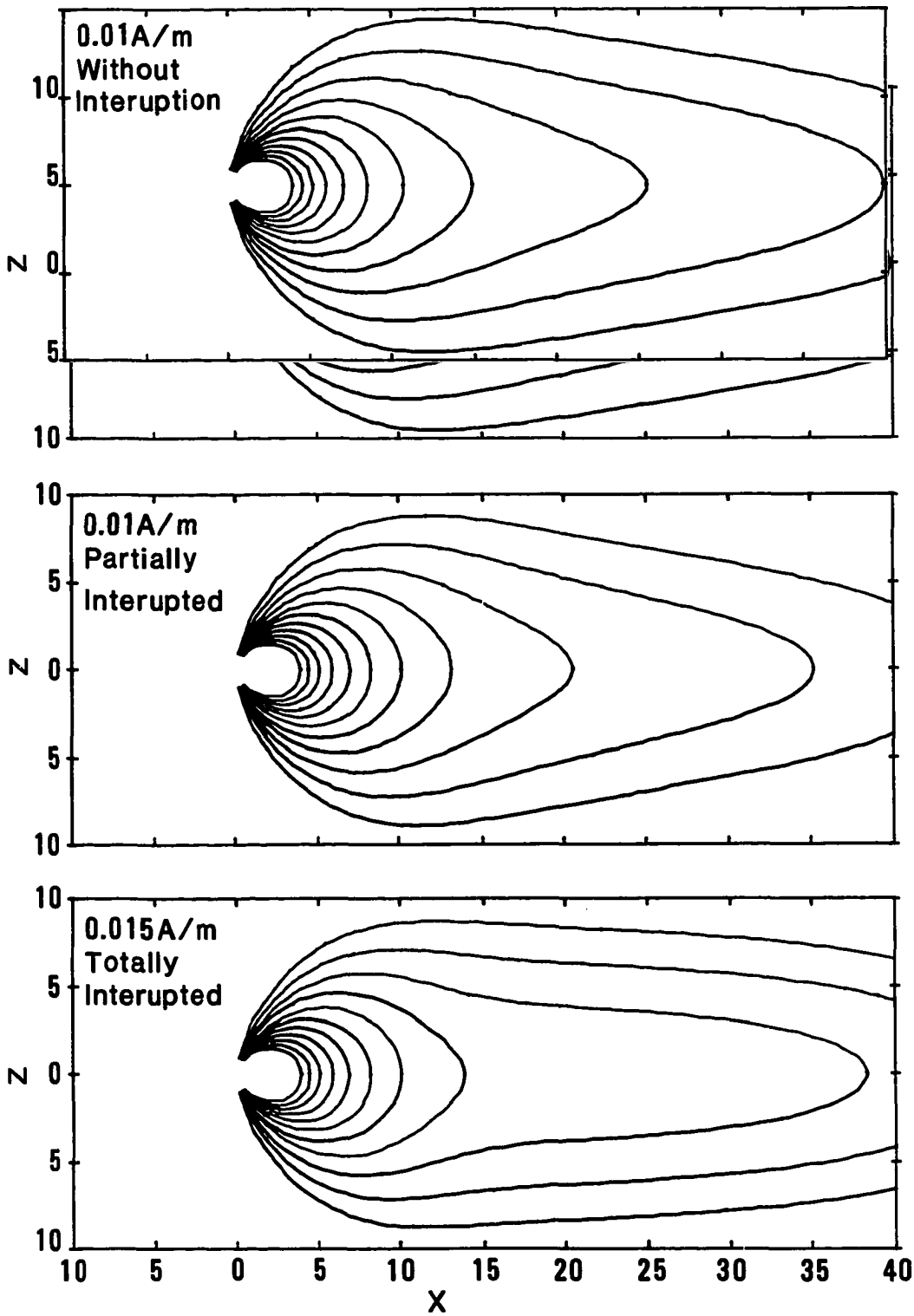

Figure 12.) Magnetospheric field model for various magnetospheric conditions (Akasofu et al. 1980).

difference in the ion and electron loss cone distributions. Because of this, there will be a local field aligned potential [Alfven and Falthammer (1963)]. The treatment of nonadiabatic changes in the magnetic moment may be generalized to any local minimum in the magnetic field. For the single particle case, there is no difference between a spacial and temporal minimum in the magnetic field. Thus, for the general case where $\underset{\sim}{B} = \underset{\sim}{B}(t)$, there will be additional nonadiabatic effects from the temporal changes in the magnetic field. Since the single particle technique ignores collective particle interactions and particle field interactions, a numerical simulation would answer two important questions. First, by calculating the flux of particles out of the sheet it would be possible to tell whether diffusion from this type of noncollisional pitch angle scattering is important compared to other loss processes in the plasma sheet. Secondly, depending on the type of simulation, it would be possible to tell if there are any electrostatic or electromagnetic effects which alter the situation significantly.

Appendix

A.) Numerical Approach to Particle Trajectories

The study of nonadiabatic effects on single particle behavior requires the numerical integration of the full, nonrelativistic, equations of motion [equation 1]. This is an ordinary differential equation of the form

$$y' = f\ (\ t,\ y\ )$$

$$y\ (t_o) = y_o\ . \tag{47.}$$

That is, an initial value problem where, $y=(\ y_1,y_2,y_3,\cdots,y_m)$, and $f=f(t,y_1,y_2,\cdots)$. For particle trajectories y is the phase space position of the particle $y=(x,y,z,v_x,v_y,v_z)$, and t is time.

There are several techniques which are widely used for the numerical solution of such a system of equations, however no single technique is superior to all others under all circumstances. In order to chose an appropriate technique it is necessary to evaluate what degree of accuracy and what sort of efficiency is required of the method. Several authors have published papers comparing the various techniques, which are of assistance in chosing a method for a given problem, Clark (1968), Crane and Fox (1969), Hull et al. (1972),

Shampine et al. (1976), and Diekhoff (1977). For the study of nonadiabatic effects we are interested in higher order perturbations in the adiabatic invariants, this requires the maintenance of a high degree of accuracy form time-step to time-step. With this in mind, the most appropriate technique for the single particle trajectory calculation is a version of rational polynomial extrapolation, introduced by Bulisch and Stoer (1966).

We will review the rational polynomial extrapolation technique, and a description of it may be found in a number of texts including Gear (1971) and Bulisch and Stoer (1980). Given equation 47 , we have some interval over which solutions are desired, (t_i, t_f), and a step size H, where H is a subset of (t_i, t_f). We now define a sequence of sub-steps h_i which we will use to obtain a sequence of approximate solutions to y(t)

$$h_i = \frac{H}{n_i} \tag{48.}$$

$$n_i \in (1, 2, 3, 4, 6, 8, 12, 16, \ldots)$$

the sequence n_i was suggested by Bulisch and Stoer (1964), to minimize the number of calculations. For each choice of n_i, and h_i we may obtain an approximate solution to y(t) by applying the modified midpoint rule

$$\eta_0 = y_0 \tag{49.}$$

$$\eta_1 = \eta_0 + \frac{h}{2} \; f \; (\; t_0, \; \eta_0 \;)$$

for i= 1, 2, 3,...,2n , and $t_i = t_0 + i\ h/2$

$$\eta_i = \eta_{i-1} + h \; f \; (\; t_i, \; \eta_i \;)$$

then,

$$\eta \; (\; t, \; h) = \tfrac{1}{2} \; (\; \eta_{2n} + \eta_{2n-1} + h/2 \;)$$

The sequence $\eta \; (\; t, \; h_k)$ represents a sequence of increasingly better approximations to y(t).

We now wish to use our initial sequence $\eta \; (\; t, \; h_k)$, of approximations to compute an increasingly better sequence of approximations to y(t). This may be done by means of a computational tableau, which we will denote $T_{i,k}$ and a recursion relation derived by Bulisch and Stoer (1964). Under the assumption that

$$T_{i,k} = \lim_{h \to 0} \tilde{T}_{i,k} \; (h)$$

where

$$\tilde{T}_{i,k}(h_j) = \eta \; (\; t, \; h_j) \qquad j= i, \; i-1, \; i-2...,i-k$$

Bulisch and Stoer extrapolated the rational function of the form

$$\tilde{T}_{i,k} = \frac{a_{i,0} + a_{i,1}h^2 + a_{i,2}h^4 + \ldots + a_{i,\mu}h^{2\mu}}{b_{i,0} + b_{i,1}h^2 + b_{i,2}h^4 + \ldots + b_{i,\nu}h^{2\nu}} \qquad (50.)$$

where $\mu = k/2$ and $\nu = k - \mu$, to find the recursion relation

$$T_{i,k} = T_{i+1,k-1} + \frac{(T_{i+1,k-1} - T_{i,k-1})}{(h_i / h_{i+k})^2 \left(1 - \frac{(T_{k+1,k-1} - T_{i,k-1})}{(T_{i+1,k-1} - T_{i+1,k-2})}\right) - 1}$$

where the first column of the tableau is $T_{1,k} = \eta(t, h_k)$. Then each successive entry in the tableau, $T_{i,k}$, is a better approximation to $y(t)$, and all that remains is to determine a condition under which we may stop the computation. This may be done simply if, given an initial step H, and an acceptable error ε, we define the relative error for each approximation $T_{i,k}$ by

$$\varepsilon_{i,k} = | T_{i,k} - y(t) | \quad . \qquad (51.)$$

It may be shown that the relative error is

$$\varepsilon_{i,k} = \left| \frac{T_{i,k} - T_{i-1,k}}{S} \right| (n_{i-k-1} / n_i)^2 \qquad (52.)$$

where $S = \max(\text{¢ } y(d) \text{¢})$; $d \varepsilon H$. All that is required is to compare the relative error at each step with the acceptable error. It should be noted that each additional row of the tableau which is computed

corresponds to an increase in the order of the rational function and in this sence the method is of "variable order".

B.) Corrections for Finite Gyroradius Effects in the Computation of the Magnetic Moment

At each time-step in the trajectory of a particle the magnetic moment is computed and compared to the previous value. If the field model under consideration varies sufficiently slowly or over large enough distances, then it is sufficient to follow the particle's position averaged over it's gyration about the magnetic field (it's "guiding center"). This notion leads to the formulation of "adiabatic theory" a review of which may be found in Northrop (1963) or Roederer (1970).

For our study of particles in the plasma sheet geometry, we are interested in the effects which occur when a particle moves from a region in which its behavior is entirely adiabatic, near the mirror points, into a region where it's behavior may be entirely nonadiabatic, near a local minimum in the magnetic field. We observe these effects by following the particle's magnetic moment which is defined in terms of the field quantities at the particle's guiding center. For the region in which the particle's behavior is adiabatic the difference between the field quantities at the particle position and the guiding center postion is insignificant, so that we may use these values to calculate the

magnetic moment. However, in the nonadiabatic region field quantities at the particle position may vary drastically from those at the guiding center position, hence we must calculate the guiding center position in order to obtain the proper field values for the calculation of the magnetic moment.

At each time-step in the particle trajectory we have the particle position, which we denote $\underset{\sim}{r}$, and the particle velocity $\underset{\sim}{v}$. To properly calculate the magnetic moment we require the field quantities at the guiding center. If we denote the guiding center position by $\underset{\sim}{R}$, and the gyroradius as $\underset{\sim}{\rho}$ $(= \overline{R\ r})$, then

$$\underset{\sim}{r} = \underset{\sim}{R} + \underset{\sim}{\rho} \tag{53.}$$

where

$$\underset{\sim}{\rho} = \frac{m\ \underset{\sim}{B}}{q\ B^2} \times \left(\underset{\sim}{v} - \frac{\underset{\sim}{E} \times \underset{\sim}{B}}{B^2} \right)$$

or in our nondimensional system,

$$\underset{\sim}{\rho}^* = \frac{\underset{\sim}{B}^*}{B^{*\,2}} \times \left(\underset{\sim}{v}^* - \frac{\underset{\sim}{E}^* \times \underset{\sim}{B}^*}{B^{*\,2}} \right) \tag{54.}$$

Then we may calculate the guiding center position form

$$\underset{\sim}{R}^* = \underset{\sim}{r}^* - \underset{\sim}{\rho}^* \tag{55.}$$

or, for example, for the plasma sheet model we get

$$\underset{\sim}{R}^{*} = \left(x^{*} + \frac{v_y^{*}}{B^{*2}} \right) \hat{i} + \left(y^{*} + \frac{(v_x^{*} - B_x^{*} v_z^{*} - E_y^{*})}{B^{*2}} \right) \hat{j} + \left(z^{*} + \frac{B_x^{*} v_y^{*}}{B^{*2}} \right) \hat{k} \quad . \tag{56.}$$

Then the magnetic moment, properly averaged over the particle gyration, may be computed from the field quantities at the guiding center postion and eqution 24 .

References

Akasofu, S. -I. and G. Corrick, A modeling of the magnetic field variations during magnetospheric substorms, Planet. Space Sci., 28, p. 749, 1980.

Alfven, H. and C.-G. Falthammer, Cosmical Electrodynamics Fundemental Principles, Oxford University Press, 1963.

Bogoliubov, N. N. and D. N. Zubarev, Ukranian Mathematical Journal VII., 1955.

Bulirsch, R. and J. Stoer, Fehlerabschatzungen und extrapolation mit rationalen funktioner bei verfahren von Richardson-typus, Num. Math., 6, p. 413-427, 1964.

Bulirsch, R. and J. Stoer, Numercial treatment of ordinary differential equations by extrapolation methods, Num. Math., 8, 1-13, 1966.

Bulirsch, R. and J. Stoer, Introduction to Numerical Analysis, Springer-Verlag, 1980.

Clark, N.W., A study of some numerical methods for the integration of systems of first order differential equations, Argon National Laboratory Report ANL-7428, 1968.

Cohen, R. H., G. Rowlands, and J. H. Foote, Nonadiabaticity in mirror machines, Physics of Fluids, 21 (4), p. 627, 1978.

Cowley, S. W. H., The adiabatic flow model of a neutral sheet, Cosmic Elect., 2, p. 90-104, 1971.

Crane, P. J. and P. A. Fox, A comparative study of computer programs for

integrating differential equations, Numer. Math. Computer Program Library One - Basic Routines for General Use, Bell Telephone Laboratories Inc., 2, No. 2, 1969.

Diekhoff, H. J. and P. Lory, H. Oberle, H. Pesch, P. Rentrop, R. Seydel, Comparing routines for the numerical solution of initial value problems of ordinary differential equations in multiple shooting, Num. Math., 27, 449-469, 1977.

Eastwood, J. W., Some properties of the current sheet in the geomagnetic tail, Planet. Space Sci., 23, 1-14, 1975.

Garren, A. and R. J. Riddell, L. Smith, G. Bing, L. R. Henrich, T. G. Northrop, and J. E. Roberts, in Proceedings of the Second United Nations International Conference on Peaceful Uses of Atomic Energy, United Nations, Geneva, 1958, 31, p 65.

Gear, C. W., Numerical Initial Value Problems in Ordinary Differential Equations, Prentice-Hall, 1971.

Grad, H. and R. Van Norton, Non-adiabatic orbits in a cusped magnetic field, Nuclear Fusion Suppl., Part 1, 61, 1962.

Hastie, R. J., G. D. Hobbs, and J. B. Taylor, in Plasma Physics and Controlled Nuclear Fusion Research, International Atomic Energy Agency, Vienna, 1969, Vol. 1, p. 389.

Howard, J. E., Nonadiabatic particle motion in cusped magnetic fields, Physics of Fluids, 14, p. 2378, 1971.

Hull, T. E. and W. H. Enright, B. M. Fellen, A. E. Sedgwick, Comparing numerical methods for ordinary differential equations, SIAM J. Num. Anal., 9, p. 603-637, 1972.

Kan, J. R., On the structire of the magnetotail current sheet, J. Geophys. Res., 78, p. 3773-3781, 1973.

Leboeuf, J. N., T. Tajima, and J. M. Dawson, Tearing, magnetic x-points, and coalescence, submitted The Formation of Auroral Arcs, Geophysical Monongraph Series, ed. S.-I. Akasofu, 1980.

Leffel, C. S., Jr. and E. P. Gray, Adiabaticity of charged-particle trajectories in a cusped magnetic field, Physics of Fluids, 12, p. 1008, 1969.

Northrop, T. G., The Adiabatic Motion of Charged Particles, John Wiley and Sons, 1963.

Pudovkin, M. I. and N. A. Tsyganenko, Particle motions and currents in the neutral sheet of the magnetospheric tail, Planet. Space Sci., 21, p. 2027-2037, 1973.

Roederer, J. G., Dynamics of Geomagnetically Trapped Radiation, Springer-Verlag, 1970.

Shampine, L. F. and M. K. Gordon, Computer Solution of Ordinary Differential Equations, the Initail Value Problem, Freeman, 1975.

Sonnerup, B. U. O., Adiabatic particle orbits in a magnetic null sheet, J. Geophys. Res., 76, p. 8211-8222, 1971.

Speiser, T. W., Particle trajectories in model current sheets - I. Analytical solutions, J. Geophys. Res., 70, p. 4219-4226, 1965.

Speiser, T. W., Particle trajectories in model current sheets - II. Application to auroraes using geomagnetic tail model, J. Geophys. Res., 72, 3919-3932, 1967.

Stern, D. P. and P. Palmadesso, Drift free magnetic geometries in

adiabatic motion, J. Geophys. Res., 80, p. 4244-4248, 1975.

Stern, D. P., Adiabatic particle motion in a nearly drift free field: applications to the geomagnetic tail, Goddard Space Flight Center Report X-602-77-89, 1977.

Swift, D. W., The effect of the neurtal sheet on magnetospheric plasma, J. Geophys. Res., 82, p. 1288-1292, 1977.

Wagner, J. S. and J. R. Kan, S.-I. Akasofu, Particle dynamics in the plasma sheet, J. Geophys. Res., 84, No.A3, 1979.

Wagner, J. S. and P. C. Gray, J. R. Kan, T. Tajima, S.-I. Akasofu, Particle dynamics in reconnection field configurations, Planet. Space Sci. (in press), 1981.